6.1 LIQUID METAL COMPATIBILITY

S. J. Pawel (Oak Ridge National Laboratory)

OBJECTIVE

The objective of this task is to identify potential structural materials having sufficient compatibility with flowing Pb-Li eutectic that the maximum metal temperature for operation can be increased to improve overall system efficiency.

SUMMARY

Operation of the first thermal convection loop (TCL) using dispersion strengthened FeCrAl (Kanthal APMT) tubing and specimens was completed in this reporting period. The working fluid in the TCL was eutectic Pb-17at%Li, and the peak temperature (550˚) and temperature gradient (116˚C) was maintained without interruption for 1000 h. When operation was terminated, a problem with complete draining of the Pb-Li from the loop was encountered, which delayed retrieval of specimens exposed in the hot leg of the TCL; however, analysis of specimens from the cold leg has been initiated.

PROGRESS AND STATUS

Introduction

Currently, the maximum allowable wall temperature for the dual coolant lead-lithium (DCLL) blanket concept is set at 475˚C based primarily on corrosion limitations of the structural containment materials. To increase overall system efficiency, potential structural materials are being sought with a combination of high strength and creep resistance with simultaneous resistance to dissolution in eutectic Pb-Li at temperatures > 500˚C. Preliminary research using static capsule exposures has indicated that dispersion strengthened FeCrAl (Kanthal APMT) may be resistant to dissolution in eutectic Pb-Li at temperatures in the range of 600-800˚C, at least in part due to the stability of an Al-rich oxide film. However, corrosion data in a flowing system must be generated to analyze the potential for issues associated with thermal gradient mass transfer – relatively high dissolution in hotter portions of the flow system with concomitant deposition in the colder portions – which has been known to disrupt heat transfer and even plug flow paths completely in some temperature gradient/material combinations.

Thus, thermal convection flow loops (TCLs) are being incorporated as the follow-on step to capsule testing for evaluation of liquid metal compatibility. The initial laboratory testing associated with this effort utilized a mono-metallic TCL fabricated of Kanthal APMT with APMT specimens inserted within each of the hot leg and cold leg of the TCL for use in post-exposure evaluation. Fabrication of the first such TCL utilizing APMT tubing (26.7 mm OD, 3.1 mm wall), which evaluated welding and heat treatment procedures to be used in subsequent TCL construction with this alloy, was successfully completed in the prior reporting period.

Results

Figure 1 shows a schematic of the APMT loop alongside a photo of the loop just prior to operation. The loop was about 1 m tall and 0.5 m wide in the flow path. Heating on one side of the loop (the “hot” leg) caused the density of the liquid Pb-Li material to decrease relative to the liquid in the unheated leg; the density difference drives flow (down on cooled side, up on heated side) once a steady temperature gradient is established. [In the schematic diagram, the liquid metal flow direction would be counterclockwise.] The loop contained two specimen chains – one in each vertical leg of the loop. Test coupons of APMT were prepared in the form of miniature tensile specimens which were strung together with APMT wire (see Figure 2). Most of the APMT test specimens received the same high temperature

oxidation treatment afforded the loop itself (slow cooled following 8 h in air at 1050˚C), but a few of the specimens were exposed in the as-machined (no oxide) condition to permit ready comparison of compatibility with Pb-Li as a function of temperature around the loop. In addition to APMT coupons, a few small rectangular specimens of commercially pure tungsten were used at the bottom of each specimen chain to act as a "sinker" to keep the relatively low density specimen chains from floating in the Pb-Li test fluid, and to act as "spacers" to keep the specimen chain centered within the tubing and liquid metal flow path.

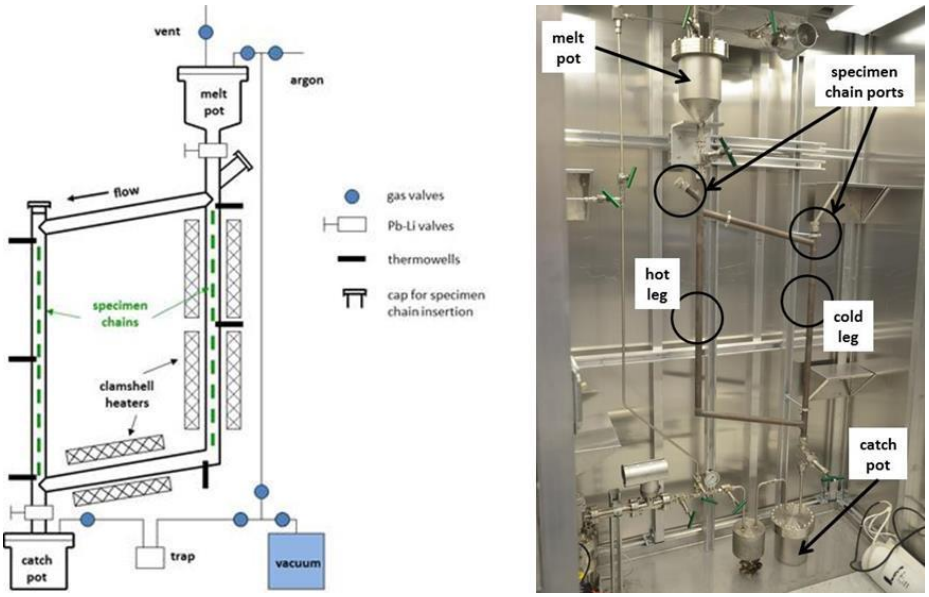

Figure 1. Schematic of the thermal convection loop for Pb-Li experiments and a photo of the actual loop prior to installation of furnaces and insulation. Actual dimensions are approximately 1 m x 0.5 m in the liquid metal flow path around the loop.

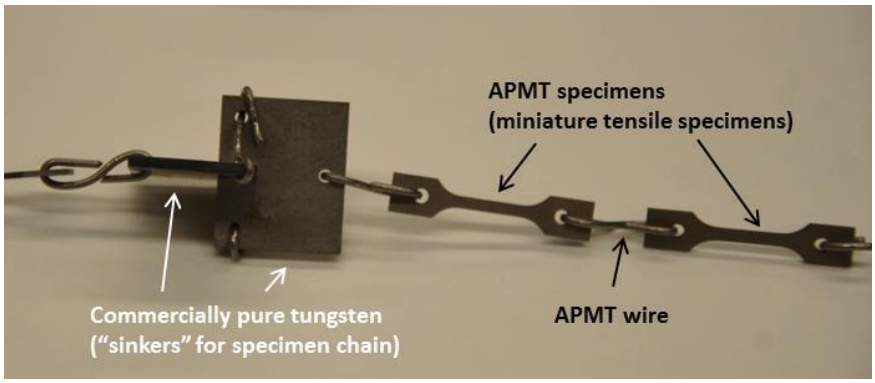

Figure 2. Representative portion of a specimen chain showing APMT miniature tensile specimens ("SS3" design) wired together (also APMT) and pieces of tungsten acting as "sinker" weights and as spacers to assure centering of the specimen chain within the tube. The tensile specimens are about 25 mm long, 5 mm wide, and 1 mm thick.

Table 1 shows the average temperatures achieved at each measurement position around the loop, which were thermowells that protruded about 0.3 cm into the flow path of the working fluid. Following stabilization of the loop (minor adjustments to heaters and insulation over the first 24 h or so), the temperatures at each position remained constant (± 1˚) at the average values for 1000 h until the loop operation was terminated.

Table 1. Average temperatures recorded at ley thermocouple positions around the loop.

Loop Position	Temperature (˚C)
Top of Hot Leg	550
Middle of Hot Leg	484
Bottom of Hot Leg	456
Top of Cold Leg	496
Middle of Cold Leg	461
Bottom of Cold Leg	434

The flow rate within the loop was estimated twice during the 1000 h operation interval using a “hot spot” test. In this evaluation, a small section of insulation on the approximately horizontal section of the loop was removed to expose the loop tubing. Next, the flame of a gas torch was held within 2-3 cm of the exposed tubing for a period of about 15 seconds to increase the Pb-Li temperature significantly in a very localized volume of material. Subsequently, as the P-Li flowed around the loop, a brief temperature spike was detected at each thermocouple location in sequence, and the time required for the temperature spike to travel the distance between detection points was used to estimate the flow rate. Figure 3 is a representative example of data collected in this manner, which displays the modest temperature spike at each location in sequence around the loop. Using this method, the flow rate was estimated to be approximately 0.4 m/min at both measurement events. This value is somewhat lower than that observed in this laboratory for recent TCLs of the similar size/design and temperature gradient utilizing sodium as the working fluid, which exhibited flow rates between 0.8-0.9 m/min. Significantly, the density difference of sodium between 450 and 550˚C (roughly the temperature gradient of interest) is 2.9% while it is only 1.7% for Pb-Li over the same temperature range. As a result of a ~ 70% greater density change, flow rate should be somewhat faster for Na compared to Pb-Li, but flow rate incorporates factors other than fluid density.

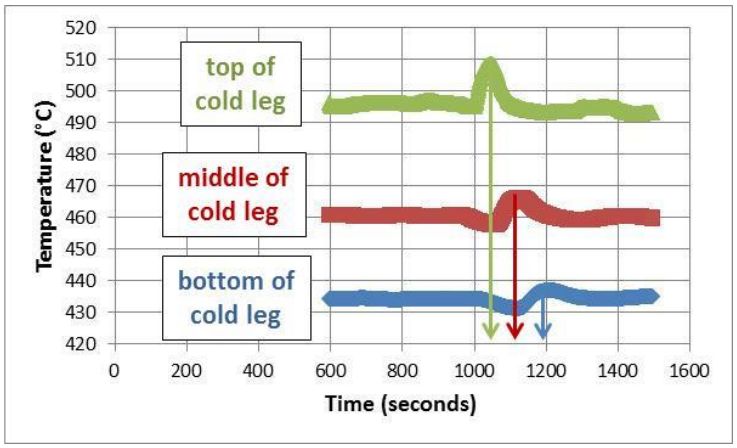

Figure 3. Representative example of data collected in "hot spot" test to estimate flow velocity of Pb-Li within the TCL.

The data in Figure 3 reveal another feature of the hot spot test. Note that for each of the cold leg positions indicated, the temperature decreases slightly prior to the temperature increase associated with the hot spot. The reason is that the application of the hot spot flame decreases the flow rate temporarily due to the imbalance created in liquid metal density at the top portion of the loop. As a result of this flow disruption, the Pb-Li in the cold leg spends a few more seconds there than normal and thus cools a few more degrees than normal. As soon as the flame is removed, however, normal flow is quickly re-established, and the hot spot travels around the loop immediately preceded by a slight dip in temperature.

Following 1000 h of operation, the loop was terminated with the initial attempt to drain the loop of Pb-Li into the dump tank positioned at the bottom of the cold leg. Unfortunately, problems were encountered with a cold spot within the very thick lid of the dump tank. After allowing all of the remaining Pb-Li to freeze in place within the loop, it was confirmed that the Pb-Li froze in this cold spot location after only partially draining from the loop. Other difficulties were encountered upon reheating of the loop to liquefy the Pb-Li and again attempt to drain it from the loop, including a small leak that developed – apparently in the thermowell weld at the top of the cold leg (analysis just beginning) – and a somewhat surprising incomplete draining of the hot leg (despite thermocouple data indicating drainage had occurred). The latter difficulties have delayed removal of specimens from the hot leg of the TCL, but analysis of cold leg specimens has begun. Curiously, the activities designed to complete removal of the hot leg specimens seem to suggest the possibility that the specimen chain, rather than hanging straight in "single file" orientation, is perhaps in a knot at about the midpoint of the hot leg. If this is confirmed, it would potentially account for reduced flow rate via adding substantial flow resistance at this location within the TCL.

Cold-leg specimens were soaked in cleaning solution (1:1:1 mixture of ethanol, hydrogen peroxide, and acetic acid) while within the loop (as an assembled chain) and again upon removal from the loop (as individual specimens). The cleaning solution readily dissolves residual Pb-Li rendering weight change measurements more meaningful. Following exposure to the cleaning solution, the specimens were ultrasonically cleaned in acetone followed by air drying prior to photography and weighing.

Figure 4 shows the mass change as a function of temperature (position) for the cold leg specimens following cleaning. The approximate temperature of each specimen location was estimated by linear extrapolation as a function of position between thermowell locations at which the temperature was known. Weight change from two starting points is given in Figure 4; that based on original (as-received) specimen weight, and that based on specimen weight following a pre-oxidation heat treatment intended to form an aluminum-rich oxide on the surface (same treatment as received by the completed loop). It is

plotted both ways (slopes of the weight change are identical) to emphasize the fact that all specimens except the one at the bottom of the cold leg reveal a net weight loss, but the total weight loss is less than the mass gained as a result of the pre-oxidation step for temperatures below about 473˚C.

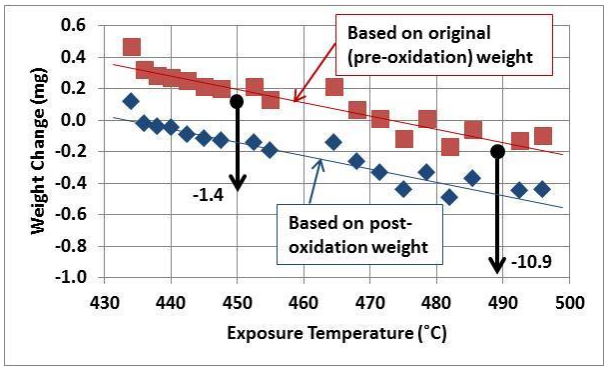

Figure 4. Weight change of specimens as a function of exposure temperature in the Pb-Li thermal convection loop. Black/round points correspond to specimens that were not given the pre-oxidation heat treatment.

The values of net weight change for the heat treated APMT specimens are quite modest. The highest weight loss, approximately 0.5 mg, can be converted to an average uniform dissolution rate using specimen density (~ 7.2 g/cm^3), specimen area (2.0 cm^2), and exposure time (1000 h), which yields a value of approximately 3 µm/y (0.1 mil/y).

Also shown in Figure 4 are the data points for two APMT specimens that were exposed without the pre-oxidation treatment afforded the rest of the specimens and loop tubing. Note that the weight loss for these specimens is a strong function of temperature – much more weight loss at the higher temperature – and substantially greater than the oxidized specimens immediately adjacent to the as-received specimen. An estimate of the uniform dissolution rate for the specimen with no pre-oxidation treatment exposed at 489˚C (10.9 mg net weight loss) yields a dissolution rate more than 25 times higher than that of the surrounding specimens. This indicates that the pre-oxidation treatment to develop aluminum oxide is an important feature of the compatibility of APMT with PbLi at these temperatures.

Note that, as in all TCL experiments, the weight change of any individual specimen is determined by the competition between dissolution activity and precipitation reactions. Additional analysis of the cold leg specimens – and the hot leg specimens when they are retrieved – will be necessary to determine additional compatibility characteristics.

Figure 5 shows the cold leg specimens after cleaning. Note that all of the specimens have varying degrees of discoloration, suggesting variable degrees of oxide film removal and/or variable degrees of deposit quantity or composition. In a qualitative sense, the relatively dark areas on each cold leg specimen seem to be relatively adherent (light scraping with sharp tweezers does not remove material), but in this manner some material is removed from the specimens without a pre-oxidation heat treatment, again suggesting a potentially significant consequence of the pre-oxidation treatment. The variable appearance of the specimens further emphasizes the need for surface analysis and metallurgical examination following tensile testing of the specimens.

Figure 5. Appearance of cold leg specimens following 1000 h exposure and cleaning. Approximate exposure temperature is given adjacent to each specimen. The specimen slightly out of line with the array of specimens is one that was not given a pre-oxidation heat treatment prior to exposure.

As funding allows, additional analysis will be pursued on all specimens (weight change, tensile testing, cross-section metallography, and SEM/microprobe assessment) as they become available.